Optimization of Control System for Electromagnetic Heating Cigarette Device

Optimization of Control System for Electromagnetic Heating Cigarette Device

Zhiqiang LI [1], Zhaoyuan LI [2], Mingqiang GUO [3], Junheng YOU [1], Shoubo LI [1], Yi HAN [1], Donglai ZHU [1], Tinghua LI [1*]

[1] Technology Center, China Tobacco Yunnan Industrial Co., Ltd., Kunming 650231, Yunnan, China;

Faculty of Information Engineering and Automation, Kunming University of Science and Technology, Kunming 650500, Yunnan, China;

[3] Changde Tobacco Machinery Co., Ltd., China Tobacco Machinery Group, Changde 415000, Hunan, China

*Corresponding author's e-mail: tinghua_li@aliyun.com

Abstract. To solve the problems of electromagnetic heating cigarette devices in heating speed and temperature control accuracy, the optimization of the control system was carried out based on the current device. And the special control system for the electromagnetic heating cigarette device was designed, which was powered by a lithium battery device and designed with a half-bridge push-pull double resonant capacitor. According to the test, the prototype can preheat at 350 ℃ in 7 seconds at the fastest, with an average rate of 44.33 ℃/s; The maximum temperature deviation at the constant temperature stage cannot exceed 5 ℃, and the temperature control accuracy can be ± 1.47%; in the simulated suction stage, the prototype can be warmed back from 280 ℃ to 340 ℃ in 3 seconds. Compared with the original dual-tube single-capacitor resonant circuit, it has nearly double the heating power. The experimental data shows that the temperature rise rate and temperature control accuracy was significantly improved, giving full play to the performance advantages of electromagnetic heating.

1. Introduction

Heated tobacco products achieve precise control of tobacco component release by heating rather than burning tobacco with exogenous heat, and meet the sensory needs of consumers based on reducing tobacco health risks. The US Food and Drug Administration approved it to be marketed as a "risk-weakened tobacco product", which is one of the most promising new tobacco products in the world [1]. The heating control system of cigarette sets is the main factor that affects the sensory quality and user experience of heated tobacco products and is the key and difficult point of the industry for a long time. Electromagnetic induction heating technology is an advanced heating technology currently applied to heated tobacco products. It has the technical advantages of a fast heat transfer rate and uniform heating and has significantly improved the comprehensive performance of products. Electromagnetic heating cigarette sets generate an eddy current in the heating element through electromagnetic induction, and the eddy current makes the element generate heat energy, thus realizing the heating of tobacco products [2]. Domestic and foreign tobacco enterprises have invested in research and development, and some products have been listed [3-8]. However, at present, the control system for electromagnetic heating cigarettes still has deficiencies in heating speed and temperature control accuracy, which affects the use

performance and sensory experience of heated tobacco products [9]. Given the above shortcomings, based on the existing system, this research adopts a lithium battery device power supply and half-bridge push-pull dual resonant capacitor design to optimize the electromagnetic heating control system and develop a special control system for electromagnetic heating cigarette sets. Compared with the original dual-tube single-capacitor resonant circuit system, the temperature rise rate and temperature control accuracy are significantly improved, giving full play to the performance advantages of electromagnetic heating in the field of heated tobacco products.

2. Main working circuit optimization

The electromagnetic heating control system mainly includes: a lithium battery charge and discharge management circuit, a power management circuit, MCU main control circuit, a power control circuit, a control feedback circuit, and a user interface circuit, as shown in Figure 1.

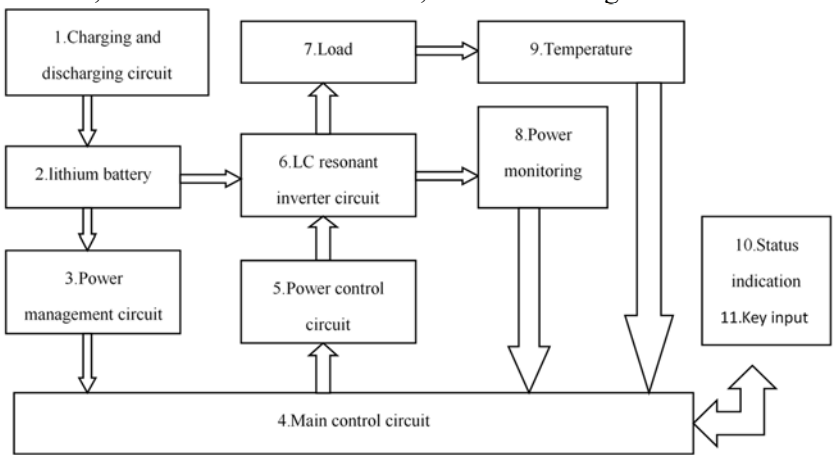

Figure 1. Overall circuit diagram of electromagnetic heating control system

The lithium battery charging circuit adopts an asynchronous boost charging controller, with a wide input voltage range (3.5V-18V), and the interface is standard TYPE-C. The charging and discharging circuit adopts the circuit shown in Figure 2. CS5086 is a dual-section lithium battery charging special chip with the function of battery power balance current, which can effectively extend the life of the battery pack. The boost switch charging converter of CS5086 has a working frequency of 500kHz and a conversion efficiency of up to 90%. Its internal integration of high-voltage transistors improves the reliability of CS5086 under various complex application conditions.

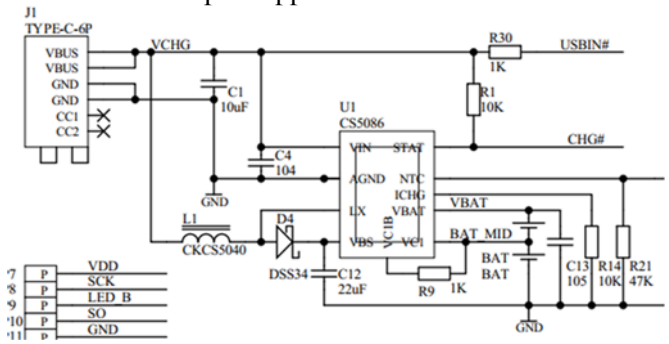

Figure 2. Charge discharge circuit

The power management circuit is shown in Figure 3. After the power circuit is opened, the main control chip is powered on and starts to work, and then the LDO is given_ EN signal to maintain the VDD power supply. When the circuit works, the main control terminal removes the LDO_ EN signal, VDD power is turned off, all control circuits, electric quantity acquisition circuits, temperature acquisition circuits, etc. are powered off and do not work, reducing the power consumption of the whole machine to the minimum. R6 and C2 in the figure form a first-order RC filter, which can filter the

fluctuation of power supply voltage caused by LC resonator operation, provide a stable input voltage for chip U2, and ensure the stability and accuracy of VDD.

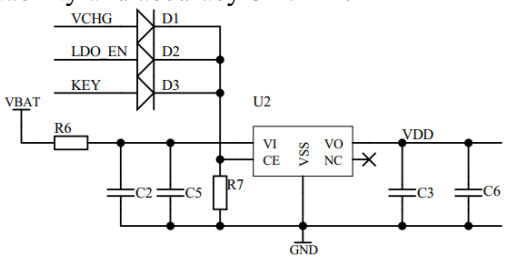

Figure 3. Power management circuit

The main control circuit uses Xin Tang N76E003 as the core controller and provides a variety of special function modules, including 256 bytes of SRAM and 768 bytes of XRAM. Up to 18 standard pins. The power circuit is realized in the form of a half-bridge driving double resonant capacitor. The dual resonant capacitor drive circuit has a higher power density than the single resonant capacitor and can achieve the specified temperature rise in a shorter time, as shown in Figure 4.

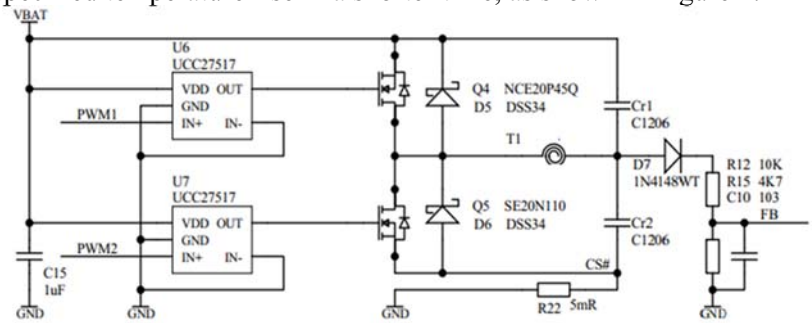

Figure 4. MOS drive and half-bridge double resonant capacitor induction circuit

In the figure, the power circuit adopts a P+N push-pull as a half-bridge drive. Driven by PWM1 and PWM2 signals, the upper and lower bridge arms (Q4 and Q5) are alternately connected to supply power to the resonant circuit composed of D5, D6, T1, Cr1, and Cr2, and the two main loops are Cr1-T1-Q5 and Q4-T1-Cr2. Since the design is powered by two series of lithium batteries, and the half-bridge working voltage is between 6.5V-8.4V, the design adopts P+N form. Compared with the N+N form, there is no need to drive the bootstrap circuit of the upper bridge arm, which simplifies the circuit design. The power circuit is driven by a 100kHz sine wave. Due to the high switching frequency and the operating voltage of the MCU is 3.3V, it is impossible to directly drive the two MOS tubes of the upper and lower bridge arms. Therefore, two additional UCC27517 are needed as MOS drive circuits. U6 and U7 are single-channel gate drivers UCC27517 launched by Texas Instruments (TI). They are a 5-pin SOT-23 small package, support a wide working voltage of 4.5V to 18V, and can ensure electrical parameters at a temperature of - 40 ℃ to 140 ℃. The maximum input voltage independent of VDD can simplify the bias power architecture. Support 4A source/pole peak current pulse, support 13ns fast typical propagation delay and 9ns/7ns rise and fall time, and realize extremely low pulse distortion; The 0.005 Ω pull-down resistance can not only minimize the switching loss when the power switch is switched through Miller Plateau, but also improve the immunity when Miller is switched on. Diode D7, voltage divider R12, R15, and capacitor C10 constitute the resonant waveform peak detection circuit.

As shown in Figure 5, a K-type thermocouple is used as the temperature feedback detection device in the temperature feedback circuit. According to the principle of thermocouple temperature measurement, the output thermoelectric potential of the thermocouple is not only related to the temperature at the measuring end but also related to the temperature at the cold end. Due to the nonlinearity of thermocouples, in the past, microprocessor tabular method or linear circuit method were used to reduce the measurement error caused by the nonlinearity of thermocouples, but these increased the difficulty of programming and debugging the circuit. The parameters of MAX6675 internal components have been precisely adjusted by laser modification technology so that the nonlinearity of

the thermocouple has been internally corrected [10] to meet the requirements. At the same time, the cold junction compensation circuit, nonlinear correction circuit, and broken wire detection circuit integrated into MAX6675 bring great convenience to the use of a K-type thermocouple.

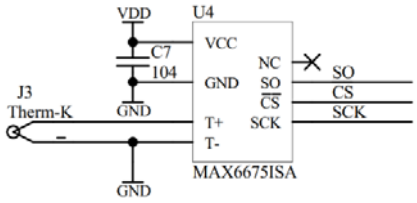

Figure 5. K-type thermocouple temperature measuring circuit

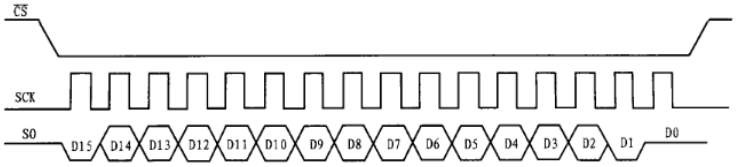

Fig. 6 MAX6675 sequence diagram

As shown in Figure 5, MAX6675 can communicate with microprocessors or other digital systems through a 3-wire serial port, and its working sequence is shown in Figure 6. When the CS pin of MAX6675 changes from high level to low level, MAX6675 will stop the conversion of any signal and output the converted data under the action of clock SCK. On the contrary, when CS changes from a low level to a high level, MAX6675 will perform a new conversion. When the CS pin changes from high level to low level, the first byte D15 will appear at pin SO. A complete data reading process requires 16 clock cycles, and data reading is usually performed at the falling edge of SCK. The output data of MAX6675 is 16 bits, of which D15 is always useless, D14~D3 corresponds to the digital conversion of analog input voltage of the thermocouple, D2 is used to detect whether the thermocouple is disconnected (D2 is 1 indicating that the thermocouple is disconnected), D1 is the identifier of MAX6675, and D0 is tristate [11]. It should be pointed out that in the previous thermocouple circuit design, a special wire break detection circuit is often needed, and MAX6675 has integrated the wire break detection circuit into the chip, thus simplifying the circuit design.

3. Parameter design of resonant circuit

In production, the resonant circuit with an inductance coil and capacitor in parallel is often used. The inductance coil is in series with resistance, and the capacitor can be used as an ideal capacitor element due to its small loss. The equivalent impedance Z of the circuit is:

$$Z=\frac{1}{\frac{1}{\mathrm{j}\omega L+R}+j\omega C}=\frac{1}{\frac{R}{R+(\omega L)}+j\left(\omega C-\frac{\omega L}{R+(\omega L)}\right)} \tag{1}$$

The condition to generate resonance is that the circuit behaves as a pure resistance, which requires the imaginary part of the impedance to be zero. From the above formula, the resonance angular frequency ω_0 can be calculated as:

$$\omega_0=\sqrt{\frac{1}{LC}-\frac{R}{L}} \tag{2}$$

The load resistance Z_0 is:

$$Z_0=\frac{R+(\omega_0 L)^2}{R}=R+\frac{L^2}{R}\omega_0=R+\frac{L^2}{R}\left(\frac{1}{LC}-\frac{R}{L^2}\right)\approx\frac{1}{RC} \tag{3}$$

The circuit is in a resonance state, $R \ll L$ so it can be obtained from the above formula:

$$f_0 \approx \frac{1}{2\pi\sqrt{LC}} \tag{4}$$

If the effective value of the power supply voltage is, the effective value of the current output from the power supply to the load I_0 is:

$$I_0 = \frac{E}{Z_0} = E\frac{RC}{L} \tag{5}$$

To keep the LC circuit in a resonance state, it is necessary to meet Formula 1. At the same time, it is necessary to achieve uniform heating of the whole heating body. The magnetic field generated by the induction coil should be evenly distributed on the whole heating body as far as possible, which requires that the induction coil should have sufficient length. According to the multi-physical field simulation results of electromagnetic heating, the inductance of the LC resonant circuit is 1.2μH. Resonant capacitance 2.2μF has a high-temperature rise rate and working efficiency. According to the size of the cigarette set system, 0.5mm enameled wire is selected, and double wire is used for 12 turns, which can cover the whole heating body. At this time, the resonant inductance is about: L=KμN2S/l=1.2μ H. According to the design power circuit working at 100kHz, the optimal efficiency point is reached when the LC resonant frequency is consistent with the working frequency under ideal conditions, and C≈2.1 is calculated according to formula 4μF. Select a similar capacity of 2.2μF. Since the LC circuit is constantly in charge and discharged during operation, the capacitor is required to have good high-frequency characteristics, temperature stability, and small size. NPO material capacitor is selected.

PID is the abbreviation of Proportional, Integral, and Differential. The PID control algorithm is the most mature and widely used in a continuous system. When tuning the parameters of the PID controller, the parameters of the controller can be adjusted by experiment according to the qualitative relationship between the parameters of the controller and the dynamic and steady-state performance of the system. To reduce the parameters that need to be adjusted, the PI controller is first used during debugging. Due to the large current of the electromagnetic heating module during operation, to ensure the safety of the system, relatively conservative parameters should be set at the beginning of commissioning, the proportional coefficient should be set smaller, and the integration time should be fixed at 0.25s, to avoid the abnormal situation that the system is unstable or the overshoot is too large to burn the electrical circuit components. The pre-set preheat temperature rise curve value is given, the system performance information is obtained according to the obtained temperature rise curve waveform, and the PID parameters are adjusted repeatedly according to the relationship between the PID parameters and the system performance. If the overshoot of the response is too large to be stable or unstable after several oscillations, the proportional coefficient should be reduced and the integration time should be increased. If the step response has no overshoot, but the controlled quantity rises too slowly and the transition time is too long, the parameters should be adjusted in the opposite direction. The preheating overshoot at the initial stage of commissioning is shown in Figure 7.

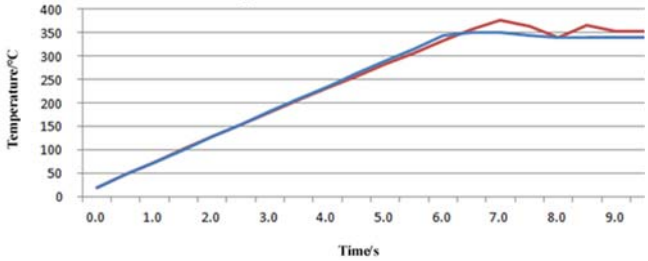

Figure 7. Preheating overshoot at the initial stage of commissioning (Blue curve: Pre-set temperature rise; Red curve: Actual temperature rise)

Because the integral time is fixed, the system needs to repeatedly adjust the proportional coefficient, fine-tune the pre-set temperature rise curve, and the overshoot is still large after many tests. Gradually add differential control, and the differential time gradually increases from 0, and repeatedly adjust the

parameters of the proportional and differential parts of the controller. The final result is shown in Figure 8.

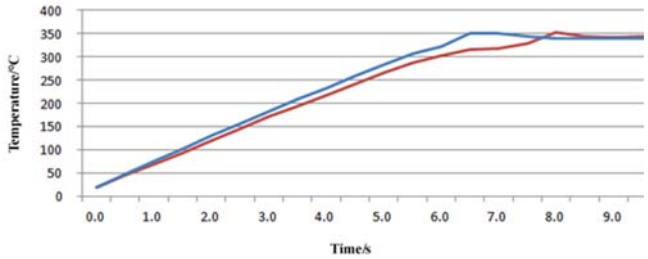

Figure 8. Pre-set curve (Blue) and actual temperature rise curve (Red) are controlled by PID

4. Experiment and discussion

According to the above design parameters, five sets of electromagnetic heating cigarette sets were developed to test the temperature rise rate and temperature control accuracy. Table 1 records the time required for five test prototypes to rise from normal temperature to the preset temperature of 350 ℃. Figure 9 shows the temperature rise test results of the electromagnetic heating cigarette control system developed in this research for prototype 1 # - 5 #. All systems reach the preset temperature (347-355 ℃) within 7-9 seconds, with an average temperature rise rate of 44.33 ℃/s.

Table 1 Temperature rise test results of electromagnetic heating cigarette set the prototype

No.	Maximum temperature/ (℃)	Heating time/ (s)
1#	352	8.0
2#	347	7.0
3#	354	9.0
4#	352	8.0
5#	349	9.0

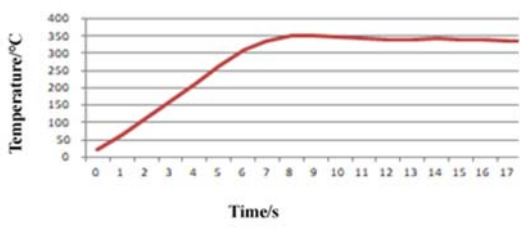

(a) 1# preheating temperature rise curve

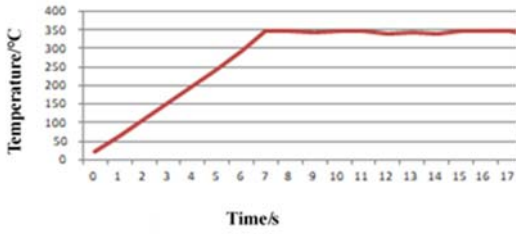

(b) 2# preheating temperature rise curve

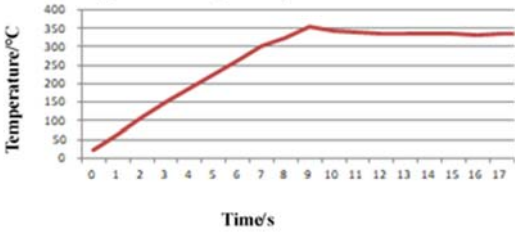

(c) 3# preheating temperature rise curve

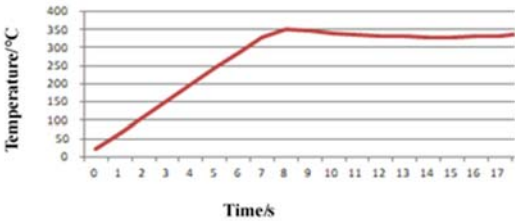

(d) 4# preheating temperature rise curve

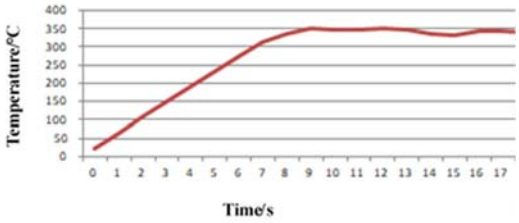

(e) 5# preheating temperature rise curve

Figure 9. The preheating curve of prototype 1 # to 10 #

Conduct a 340 ℃ constant temperature test on five prototypes, and record the results in Table 2. It can be seen from the table that the maximum temperature deviation of the five prototypes is not more than 5 ℃, and the temperature control accuracy is within ± 1.47%. Figure 10 shows the temperature fluctuation measured after the five prototypes enter the constant temperature stage after the completion of preheating.

Table 2 Constant temperature test results

No.	Thermostatic maximum temperature/ (℃)	Thermostatic minimum temperature/ (℃)	Maximum fluctuation value/ (℃)
1#	344	335	5
2#	343	336	4
3#	343	336	4
4#	344	336	4
5#	343	336	4

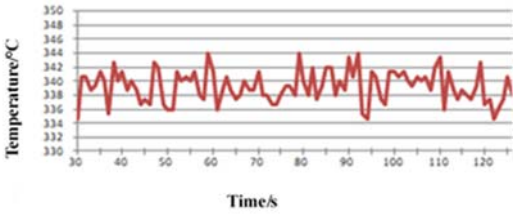

(a) 1# constant temperature fluctuation curve

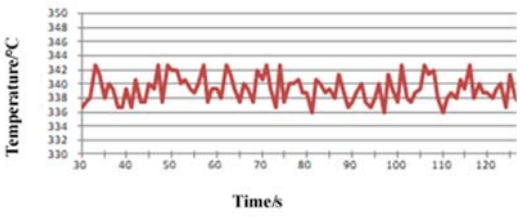

(b) 2# constant temperature fluctuation curve

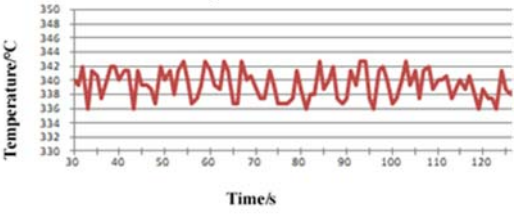

(c) 3# constant temperature fluctuation curve

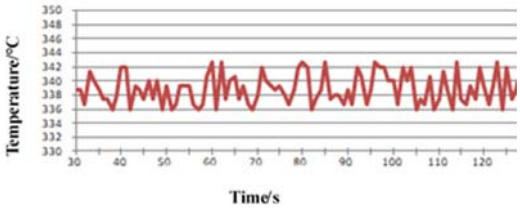

(d) 4# constant temperature fluctuation curve

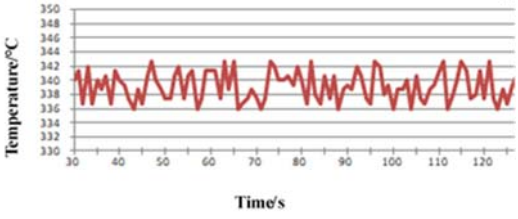

(e) 5# constant temperature fluctuation curve

Figure 10. Temperature fluctuation of 5 prototypes at constant temperature stage

During the suction process, due to the influence of the external airflow, the heating temperature of the system will drop suddenly. At this time, the system is required to quickly recover the temperature to the pre-set value after each mouthful is smoked to maintain the consistency of the suction taste of the heated tobacco products. Therefore, the temperature recovery speed is also one of the main indicators to measure the performance of the control system. Simulated suction and temperature return speed tests were conducted on five prototypes, and the results are shown in Figure 11. During pumping, the heat of the heating element is taken away, and the temperature drops rapidly to below 290 ℃. The control system detects that the temperature drops rapidly, and the control power circuit increases the power output to quickly warm the heating element. The temperature of the five systems decreased to an average of 278.4 ℃ during suction, the temperature return time was within 4 s, and the average temperature return speed was 17.0 ℃/s, which met the design requirements of the system.

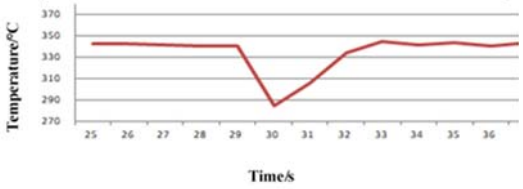

(a) 1# temperature return test curve

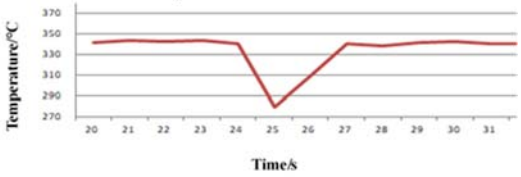

(b) 2# temperature return test curve

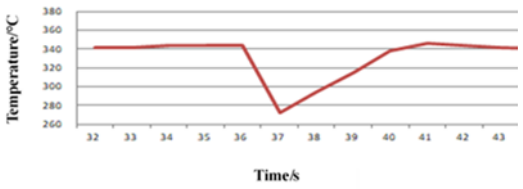

(c) 3# temperature return test curve

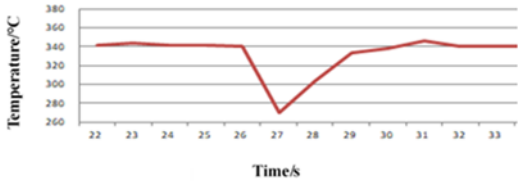

(d)4# temperature return test curve

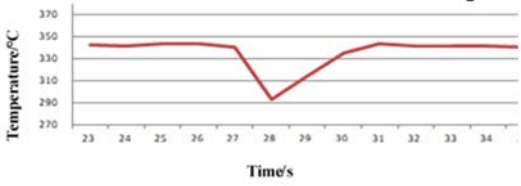

(e) 5# temperature return test curve

Figure 11. Temperature return test of 5 prototypes

5. Conclusions

The resonance modes of an electromagnetic heating system include parallel and series modes, and the control modes include single tube, double tube, push-pull, full-bridge, and other modes. The two can be combined to form a variety of heating systems according to needs. Due to the structural space limitation of the cigarette set system, the system is required to rise rapidly from normal temperature to more than 300 ℃. This research adopts the half-bridge push-pull double resonant capacitor design, which has nearly double the heating power compared with the original double-tube single-capacitor resonant circuit. By optimizing the main working circuit and designing the resonant circuit, the heating speed and temperature control accuracy of the electromagnetic heating control system is significantly improved. The test results show that the eddy current heating system can preheat at 350 ℃ in 7 seconds, with an average rate of 44.33 ℃/s; At the constant temperature stage, the maximum temperature deviation shall not exceed 5 ℃, and the temperature control accuracy shall be within ± 1.47%; in the suction stage, the system can rapidly return to 340 ℃ from 280 ℃ in 3 seconds, and the average temperature return speed is 17.0 ℃/s. The research results provide a method and data basis for the development and design of the vortex heating cigarette control system.

Acknowledgments
Financial support of the major scientific and technological special project of China National Tobacco Co., Ltd (Grant No.110202101075 (XX-20)), The science and technology plan project of Yunnan Provincial Department of Science and Technology (Grant No.202105AD160007), Science and technology project of Yunnan China Tobacco Industry Co., Ltd (Grant No.2022XY04) are greatly acknowledged.

References
[1] HAN Jingmei, ZHANG Mingjian, SHANG Shanzhai, et al. (2021) The puff-by-puff release laws of main constituents in the aerosol produced by electrically heated tobacco products with different structured filters. Acta Tabacaria Sinica, 27(01):1-7.
[2] Rudnev V I, Loveless D, Cook R, et al. (2002) Handbook of induction heating. Boca Raton：CRC Press, Florida.
[3] Bureau of international cooperation. (2015) Chinese Academy of Agricultural Sciences Theory and practice of international cooperation in agricultural science and technology in China: 2015. Beijing: China Agricultural Science and Technology Press, Beijing.
[4] JIN Zhaodan. (2020) Exploration and Research on the development trend of the packaging design of new tobacco products. Green packaging, 10: 56-63.
[5] Smith M R, Clark B, Lüdicke F, et al. (2016) Evaluation of the tobacco heating system 2.2. Part 1: Description of the system and the scientific assessment program. Regulatory Toxicology and Pharmacology, 81(2): S17-S26.
[6] Werley M S, Freelin S A, Wrenn S E, et al. (2008) Smoke chemistry, in vitro and in vivo toxicology evaluations of the electrically heated cigarette smoking system series K. Regulatory Toxicology and Pharmacology, 52(2):122-139.
[7] Mottier N, Tharin M, Cluse C, et al. (2016) Validation of selected analytical methods using accuracy profiles to assess the impact of a tobacco heating system on indoor air quality. Talanta,158(9):165-178.
[8] Baker R R. (2006) Smoke generation inside a burning cigarette: modifying combustion to develop cigarettes that may be less hazardous to health. Progress in Energy and Combustion Science,32(4):373-385.
[9] ZENG Xianqing, HAN Donglin, HUANG Yuchuan, et al. (2021) Development and the prospect of lithium-ion battery for heated tobacco products. Acta Tabacaria Sinica,27(6):112-119.
[10] HU Zhaoji, REN Aifeng, WANG Qiaoyu, XIONG Xin. (2011) Design and implementation of a multi-channel temperature acquisition system based on MAX6675. Electronic technology, 24(5):29-31.
[11] WU liming, SHI Yanjun, JIANG Hua, ZHANG Zhenkun. (2011) Automatic detection system of energy efficiency of electric rice cooker based on a virtual instrument. Automation and information engineering,32(2):10-13.